Genes & Diseases (2023) 10, 2082–2096

Available online at www.sciencedirect.com

ScienceDirect

journal homepage: www.keaipublishing.com/en/journals/genes-diseases

FULL LENGTH ARTICLE

LRP1B suppresses HCC progression through the NCSTN/PI3K/AKT signaling axis and affects doxorubicin resistance

Xiangyu Zhai [a,1], Zhijia Xia [b,1], Gang Du [a,d,1], Xinlu Zhang [c], Tong Xia [d], Delin Ma [d], Xiaosong Li [e,*], Bin Jin [a,d,**], Hao Zhang [a,d,***]

[a] *Department of Hepatobiliary Surgery, The Second Hospital of Shandong University, Jinan, Shandong 250033, China*
[b] *Department of General, Visceral, and Transplant Surgery, Ludwig-Maximilians-University Munich, Munich 81377, Germany*
[c] *Department of Reproductive Medicine, Central Hospital Affiliated to Shandong First Medical University, Jinan, Shandong 250013, China*
[d] *Organ Transplant Department, Qilu Hospital of Shandong University, Jinan, Shandong 250012, China*
[e] *Clinical Molecular Medicine Testing Center, The First Affiliated Hospital of Chongqing Medical University, Chongqing 400016, China*

Received 17 August 2022; accepted 23 October 2022
Available online 23 November 2022

KEYWORDS
Doxorubicin;
Hepatocellular carcinoma;
LRP1B;
PI3K/AKT pathway;
Tumor mutation burden

Abstract Accumulating evidence supports the association of somatic mutations with tumor occurrence and development. We aimed to identify somatic mutations with important implications in hepatocellular carcinoma (HCC) and explore their possible mechanisms. The gene mutation profiles of HCC patients were assessed, and the tumor mutation burden was calculated. Gene mutations closely associated with tumor mutation burden and patient overall survival were identified. *In vivo* and *in vitro* experiments were performed to verify the effects of putative genes on proliferation, invasion, drug resistance, and other malignant biological behaviors of tumor cells. Fourteen genes with a high mutation frequency were identified. The mutation status of 12 of these genes was closely related to the mutation burden. Among these 12 genes, *LRP1B* mutation was closely associated with patient prognosis. Nine genes were associated with immune cell infiltration. The results of *in vivo* and *in vitro* experiments showed that the knockdown of *LRP1B* promotes tumor cell proliferation and migration and enhances

* Corresponding author.
** Corresponding author.
*** Corresponding author.
E-mail addresses: lixiaosong@cqmu.edu.cn (X. Li), jinbin@sdu.edu.cn (B. Jin), 201735939@mail.sdu.edu.cn (H. Zhang).
Peer review under responsibility of Chongqing Medical University.
[1] These authors contributed equally to this work and shared the first authorship.

https://doi.org/10.1016/j.gendis.2022.10.021

the resistance of tumor cells to liposomal doxorubicin. *LRP1B* could directly bind to *NCSTN* and affect its protein expression level, thereby regulating the PI3K/AKT pathway. Our mutational analysis revealed complex and orchestrated liposomal alterations linked to doxorubicin resistance that may also render cancers less susceptible to immunotherapy and also provides new treatment alternatives.

Introduction

Liver cancer is the sixth most common malignancy and the fourth leading cause of cancer-related death worldwide.[1] Hepatocellular carcinoma (HCC) is the most common type of primary liver cancer, accounting for more than 80% of primary liver cancers worldwide.[2] Classic clinical treatments for HCC include surgery, radiotherapy, chemotherapy, and immunotherapy. Despite these diverse possible treatments, the mortality rate of HCC remains high; the 10-year overall survival rate is 10%, and the rates of local recurrence and metastasis are often high.[3]

Tumor mutation burden (TMB) reflects the number of nonsynonymous mutations in the genome and can be used to predict patient prognosis and treatment outcomes. Nonsynonymous mutations can lead to structurally distinct mutant protein products that act as neoantigens, increasing the possibility that cancer cells are recognized by cytotoxic T lymphocytes.[4] Therefore, nonsynonymous mutations have clinical significance in predicting the immunotherapy response. Through bioinformatics analysis, we found a close relationship between LDL receptor-related protein 1 B (*LRP1B*) expression and TMB; in addition, *LRP1B* mutation is associated with the efficacy of immunotherapy in multiple cancer types.[5] Therefore, *LRP1B* can be used as a biomarker to predict survival and the efficacy of immunotherapy in HCC patients.

We aimed to explore gene mutations associated with the TMB, immune infiltration, and prognosis of liver cancer. Our study showed that mutations in *TP53*, *TTN*, *MUC16*, *AHNAK2*, *OBSCN*, *FLG*, and *LRP1B* are closely related to TMB. *XIRP2*, *MUC16*, *HMCN1*, and *LRP1B* are associated with $CD8^+$ T-cell infiltration, and *LRP1B* mutation is associated with prognosis in patients with liver cancer.

LRP1B functions as a tumor suppressor gene in cancers such as prostate cancer,[6] colon cancer,[7] thyroid cancer,[8] and gastric cancer.[9] In addition, the mutation status and expression level of *LRP1B* are closely related to prognosis in various cancers.[10–12] Multiple miRNAs can promote tumor proliferation, invasion, and migration by targeting *LRP1B*.[6,13] However, the mechanism underlying the role of *LRP1B* in tumors is unclear. We identified *NCSTN* as the interacting protein of *LRP1B* by coimmunoprecipitation (co-IP), mass spectrometry, and other research methods. *LRP1B* could bind with *NCSTN* and affect its protein expression level. Furthermore, through *in vitro* and *in vivo* experiments, we found that *LRP1B* exerts a tumor suppressor effect by regulating the PI3K/AKT signaling pathway through *NCSTN*. In liver cancer, *LRP1B* could affect lipid metabolism in liver cancer cells and resistance to liposomal doxorubicin.

In conclusion, our bioinformatics analysis revealed that *LRP1B* has a high mutation rate in HCC and is closely related to tumor mutation burden and prognosis in HCC. Then, we found that *LRP1B* affects lipid metabolism, proliferation, and drug resistance in cancer cells through the NCSTN/PI3K/AKT signaling axis. Therefore, *LRP1B* could be used to predict the prognosis of liver cancer patients and the efficacy of doxorubicin treatment and immunotherapy in liver cancer patients and could be used as a potential target for immunotherapy.

Materials and methods

Mutation analysis

Genome sequencing data for 352 and 331 HCC patients were obtained from the International Cancer Genome Consortium (ICGC; daco.icgc.org) database and The Cancer Genome Atlas (TCGA; portal.gdc.cancer.gov) database, respectively. The mutation frequency and mutation type for each gene were quantitatively determined and presented as a waterfall plot. In addition, clinical information of 375 patients with liver cancer, including age, sex, TNM stage, survival time, and survival status, was obtained. Somatic mutation data were analyzed using the "maftools" R package, the TMB of the patients was calculated, and the patients were divided into the low TMB and high TMB groups. Associations between TMB and single-gene mutations were determined by analyzing mutation data from both groups of patients.

Survival analysis based on single-gene mutation status

The mutation data and clinical data of each patient were paired, and the patients were divided into mutant-type and wild-type groups according to the mutation status of every single gene. The survival curves for the two groups of patients were drawn, and the 5-year survival rates were calculated. Univariate and multivariate Cox regression analyses were performed on the mutant genes screened by survival analysis to determine whether each single-gene mutation was an independent prognostic factor.

Immune infiltration analysis

The CIBERSORT algorithm was used to calculate the patients' immune cell score.[14] The analyzed immune cells included B cells (naive B cells and memory B cells), T cells

($CD8^+$ T cells, $CD4^+$ T cells, etc.), natural killer cells, and macrophages. The patients were divided into the wild-type and mutant-type groups according to mutation status. Differences in immune cell infiltration scores between the two groups of patients were analyzed using the "vioplot" package in R software.

Gene ontology (GO) functional enrichment analysis and gene set enrichment analyses (GSEA).

Differences in gene expression between the wild-type and mutant groups of patients were analyzed. Difference analysis, normalization, and visualization of raw transcriptome data were performed with the "limma" package in R software. GO functional enrichment analysis was performed using the "enrichplot", "org.Hs.eg.db" and "ggplot2" packages in R software. GSEA was performed using software downloaded from "gsea-msigdb.org" (http://www.gsea-msigdb.org/gsea/index.jsp).

Mutation-related gene analysis and identification of potential small molecule drugs

Differentially expressed genes (DEGs) associated with single-gene mutations were analyzed using the online analysis tool muTarget (mutarget.com). DEGs were uploaded to the Connection Map (CMap) database (portals.broadinstitute.org/cmap) to identify drugs that could potentially reverse specific biological effects caused by a single gene mutation in HCC. The structures of potential small molecule drugs were obtained from the PubChem database (pubchem.ncbi.nlm.nih.gov).

Evaluation of cell proliferation ability

Cell proliferation ability was assessed using plate colony formation and Cell Counting Kit-8 (CCK-8) assays. Cells subjected to different treatments were seeded into 6-well plates (approximately 1,000 cells per well). After two weeks of culture, the cells were fixed with formaldehyde, stained with crystal violet, and photographed. A total of 10 μL/well of CCK-8 reagent (Beyotime, Shanghai, China) was added to a 96-well plate containing 2,000 cells per well and incubated at 37 °C for 2 h. The optical density values at 450 nm (OD450) were measured with a 96-well multimode plate reader (Biotech Instruments, Winooski, USA).

Evaluation of cell invasion ability

Cell invasion ability was evaluated using Transwell chambers with 8 μm-pore size polycarbonate membrane filters. After transfection for 24 h, cells were added to the upper compartments of chambers containing membranes coated with Matrigel (BD Bioscience, NJ, USA) and cultured for an additional 24 h. For the wound healing (scratch) assay, cells were seeded in 6-well plates. After the cells were confluent, a scratch was made in the monolayer, and digital images were acquired after 0, 24, and 48 h.

Apoptosis and cell cycle analyses

Transfected cells were examined 48 h post transfection. Apoptosis and the cell cycle status were then assessed using apoptosis and cell cycle kits, respectively (Beyotime, Shanghai, China). Specifically, cells were resuspended in 500 μL of binding buffer and incubated with 5 μL of FITC and 5 μL of PI (apoptosis) or PI/RNase A (cell cycle) for 15 min at room temperature in the dark. Samples were analyzed by flow cytometry (BD Accuri™C6, USA).

Cell immunofluorescence analysis

A total of 3×10^3 cells were seeded on coverslips in each well of a 24-well plate. Cells were fixed with 4% paraformaldehyde for 20 min at room temperature, permeabilized with 0.2% Triton X-100 in PBS for 10 min, blocked in 5% BSA for 1 h at room temperature, and incubated with the primary antibodies overnight at 4 °C. The cells were then incubated with fluorophore-conjugated secondary antibodies (1:1,000; Thermo Fisher Scientific, CA, USA). After washing, sections were incubated with DAPI (Beyotime, Shanghai, China), washed, and mounted. Images were acquired with a ZEISS microscope (Axio Imager A2/AxioCam HRc; Zeiss, Jena, Germany).

Western blotting (WB)

Protein was extracted with 0.5% SDS and quantified using a BCA protein estimation kit (Boster, Wuhan, China). The PVDF membrane was incubated first with the primary antibody overnight at 4 °C and then with the corresponding secondary antibodies at room temperature for 1 h. Immunoreactive bands were visualized using an ECL detection kit (Boster, Wuhan, China) and imaged with a GeneGnome5 Chemiluminescence Series Image Capture system (Syngene, Frederick, USA). Detailed information on all antibodies is shown in Table S1.

Animal model establishment

Male *BALB/c* nude mice (12–14 g, 3–4 weeks old) were obtained from Hubei Biont Bioscience. Huh7 cells (2×10^6) subjected to different treatments were suspended in 100 μL of PBS and inoculated subcutaneously into the bilateral flanks of nude mice. The tumors were measured every five days, and the volume was calculated according to the following equation: volume = length × width^2/2. One month after cell injection, the mice were euthanized, and the tumors were harvested. For immunohistochemical staining, tumor sections were incubated first with the primary antibody and then with the secondary antibody.

Huh7 cells (1×10^6 cells per mouse) subjected to different treatments were injected into *BALB/c* nude mice via the tail vein. One month after injection, the mice were euthanized, and the lungs were removed. The formation of HCC metastatic foci in the lung was confirmed by hematoxylin and eosin staining.

Co-immunoprecipitation (IP) and ubiquitination assays

The co-IP assay was performed using a Pierce Crosslink Magnetic IP/Co-IP Kit (Thermo Fisher Scientific, CA, USA) according to the manufacturer's instructions. Whole-cell

lysates were incubated with the desired antibodies, and the target protein was then pulled down with protein A/G magnetic beads. The microbeads were then washed with a lower-concentration binding buffer, which caused the bound protein to dissociate from the antibody-conjugated beads. The eluate was collected and examined by WB and SDS-PAGE. For the ubiquitination assay, cells co-transfected with the indicated plasmids were lysed in cold IP lysis buffer containing 1% SDS. Subsequently, the lysates were diluted tenfold with IP lysis buffer and subjected to ultrasonic disruption and centrifugation. The next steps were the same as those used for co-IP.

Statistical analysis

The results are presented as the mean ± standard error of the mean (SEM). Statistical analysis was performed using an unpaired *t*-test. Bioinformatic and statistical analyses were performed using the R package mentioned earlier. DEGs were identified according to the threshold $|\log_2$ (fold change)$| > 1$ and P value < 0.05. GSEA was performed using GSEA version 3.0 (Broad). For the enrichment analysis, the enrichment results were considered meaningful when the false discovery rate (FDR) was <0.05. Statistical analyses of the experimental results were carried out using SPSS version 24.0 (SPSS Inc., Chicago, IL, USA). Two-tailed P values less than 0.05 ($P < 0.05$) were considered statistically significant.

Results

Tumor mutation burden

The top 30 high mutation frequency genes from the TCGA database are shown in Figure 1A. In the ICGC database, the top 30 high mutation frequency genes included *TP53*, *TTN*, *MUC16*, *IGFN1*, and *AHNAK2* (Fig. 1B). The mutated genes and types of mutations in each patient were quantitatively determined in the TCGA and ICGC databases, and the most common type of mutation was a missense mutation (Fig. 1C, D). The results obtained in the two databases were intersected to identify 14 genes with high mutation frequencies (Fig. 1E, F). The results of correlation analysis between TMB and gene mutation status showed that the mutation status of *TP53*, *TTN*, *MUC16*, *AHNAK2*, *OBSCN*, *FLG*, *PCLO*, *LRP1B*, *HMCN1*, *USH2A*, and *XIRP2* was closely related to TMB in patients (Fig. 1G). TMB was significantly higher in patients with the above gene mutations ($P < 0.01$).

Prognostic and immune cell infiltration analyses

The patients were divided into the wild-type and mutant groups based on the mutation status, and survival analysis was performed using the Kaplan–Meier survival method (Fig. 2A–N). Patients with *LRP1B* mutation had a worse prognosis than those without *LRP1B* mutation (Fig. 2F). Univariate Cox regression analysis showed that disease stage and *LRP1B* mutation status were associated with prognosis ($P < 0.05$; Fig. 2O). Multivariate Cox regression analysis indicated that disease stage and *LRP1B* mutation were independent prognostic factors ($P < 0.05$) and that *LRP1B* mutation was associated with a poor prognosis (hazard ratio >1, $P < 0.05$; Fig. 2P). The proportion of immune cells per patient was calculated using CIBERSORT R script v1.03. $P < 0.05$ was used as the screening threshold, and the results of the immune cell infiltration analysis of 138 patients were considered reliable and used for further analysis (Fig. S1). *LRP1B* mutation was associated with the infiltration of $CD8^+$ T cells, macrophages, activated mast cells, and activated memory $CD4^+$ T cells (Fig. 2Q). Other genetic mutations were also associated with the infiltration of different immune cells (Fig. S2). GSEA was performed according to the mutation status of *LRP1B*. Mutation of *LRP1B* was associated with cellular metabolism and a variety of immune- or inflammation-related pathways, including the nuclear factor kappa-B (NF-κb) signaling pathway and the tumor necrosis factor (TNF) signaling pathway (Fig. 2R).

LRP1B mutation-related gene analysis, functional enrichment analysis, and therapeutic molecule prediction

To further analyze the biological function of *LRP1B* mutation, we identified the genes associated with *LRP1B* mutation. The expression levels of *ILRUN*, *APTR*, *TCF19*, *LOC101927021*, *TMEM14A*, *TMEM97*, *LOC730101*, and *LIMD1* were significantly higher in patients with *LRP1B* mutation. Conversely, the expression levels of *SCN1B* and *DNASE1L3* were lower in the mutant group (Fig. 3A–J). Small molecules with potential therapeutic effects against liver cancer were then predicted based on the mutation-related DEG profiles (Table S2). Serdemetan, alisertib, caffeic acid, pyrimethamine, and doxorubicin have strong therapeutic potential (Fig. 3K–O). Among these agents, doxorubicin is widely used in the treatment of liver cancer. GO enrichment analysis showed that *LRP1B* was associated with various pathways, such as the NF-κB pathway, PI3K/AKT pathway, and TNF pathway (Fig. 3P). Kyoto Encyclopedia of Genes and Genomes (KEGG) enrichment analysis showed that *LRP1B* is associated with apoptosis, membrane trafficking, cytokines, drug metabolism, and immune-related pathways (Fig. 3Q).

Low expression of *LRP1B* in hepatocellular carcinoma is associated with cell migration, proliferation, and apoptosis

Specimens were collected from 20 patients who underwent resection for liver cancer at the Second Hospital of Shandong University between January 1, 2020, and January 1, 2021, and mRNA was extracted from the tissues for qPCR analysis. In most patients, the expression of *LRP1B* was lower in tumor tissues than in adjacent tissues (Fig. 4A). The ICGC database indicated that the liver cancer cell line Huh7 was an *LRP1B* wild-type line. We extracted mRNA from different liver cancer cell lines, and the PCR results showed that the expression level of *LRP1B* in the Huh7 cell line was significantly higher than that in the other cell lines (Fig. 4B). Therefore, the Huh7 cell line was selected for the

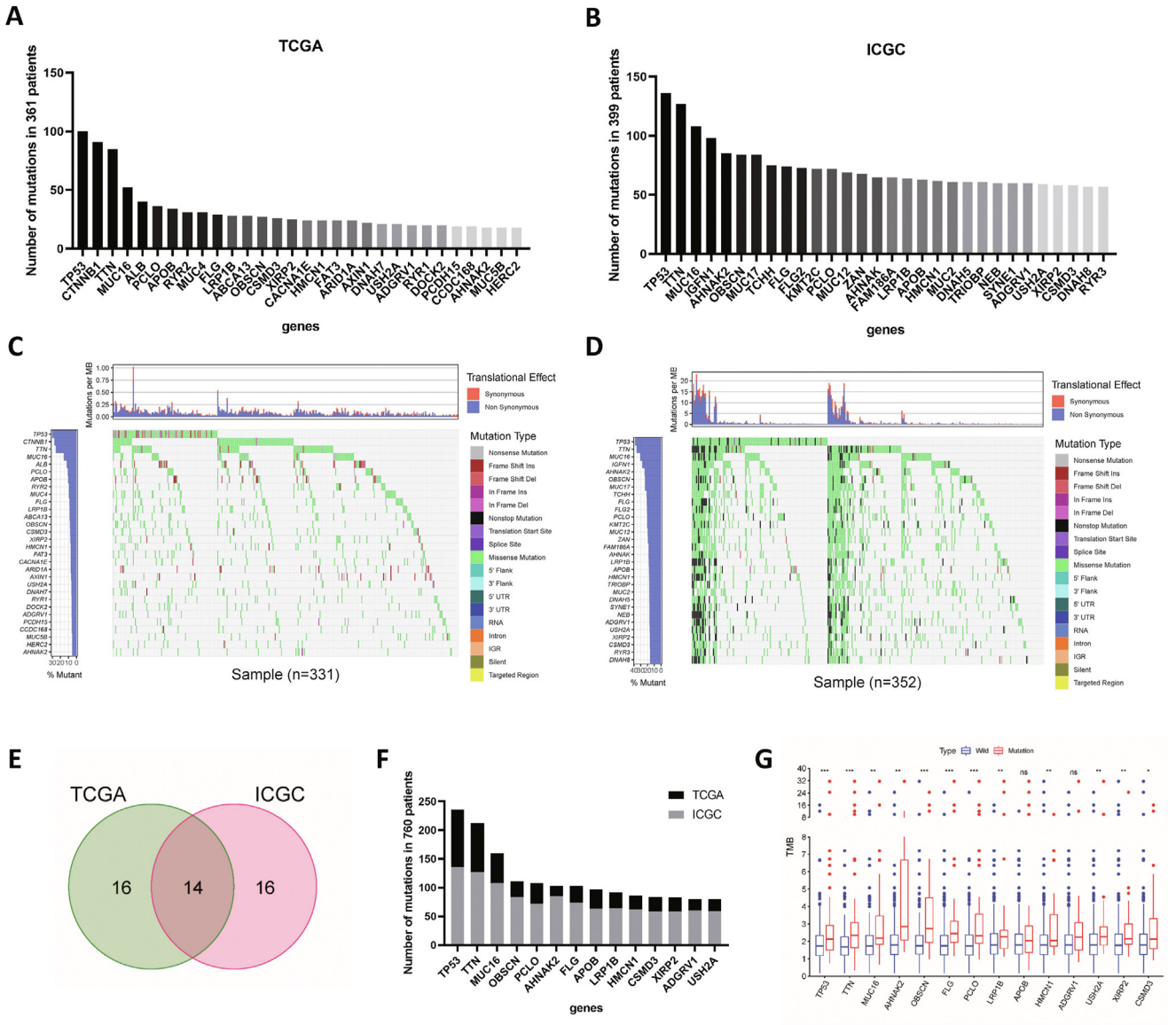

Figure 1 Gene mutation frequency statistics and screening of tumor mutation burden-related mutations. **(A)** Gene mutation frequencies in the TCGA database. **(B)** Gene mutation frequencies in the International Cancer Genome Consortium (ICGC) database. **(C)** Waterfall plot of gene mutation statuses in The Cancer Genome Atlas (TCGA) database. **(D)** Waterfall plot of gene mutation statuses in the ICGC database. **(E)** Venn diagram of mutated genes. **(F)** Mutation frequencies of the overlapping genes. **(G)** Correlation analysis of TMB and gene mutations.

functional study of *LRP1B*. Immunofluorescence analysis showed that the expression level of *LRP1B* decreased significantly after cells were transfected with *shLRP1B*. The expression level of *LRP1B* was obviously increased by *LRP1B* plasmid transfection (Fig. 4C). We employed 5-ethynyl-2′-deoxyuridine (EdU) incorporation and colony formation assays to detect the effect of *LRP1B* on cell proliferation. The percentage of EdU-positive cells was significantly higher in the *LRP1B* knockdown group (Fig. 4D). Knockdown of *LRP1B* significantly increased the colony number compared with that in the control group (Fig. 4E), suggesting that *LRP1B* knockdown increases cell proliferation. Huh7 cells with *LRP1B* knockdown demonstrated an enhanced migratory capacity (Fig. 4F). The Transwell migration assay indicated that the *LRP1B* knockdown group had a stronger migration ability than the control group (Fig. 4G). *LRP1B* knockdown led to a decrease in apoptosis upon Nutlin-3 treatment, consistent with the previous results of KEGG enrichment analysis (Fig. 4H). Flow cytometric analysis of the cell cycle showed that after *LRP1B* knockdown, the proportion of cells in the S phase increased, suggesting that cell proliferation was accelerated (Fig. 4I).

LRP1B affects tumor progression and resistance to liposomal doxorubicin *in vivo* and *in vitro*

The *LRP1B* expression plasmid or vector control plasmids were transfected separately into hepatocellular carcinoma cells. The colony formation assays further confirmed that

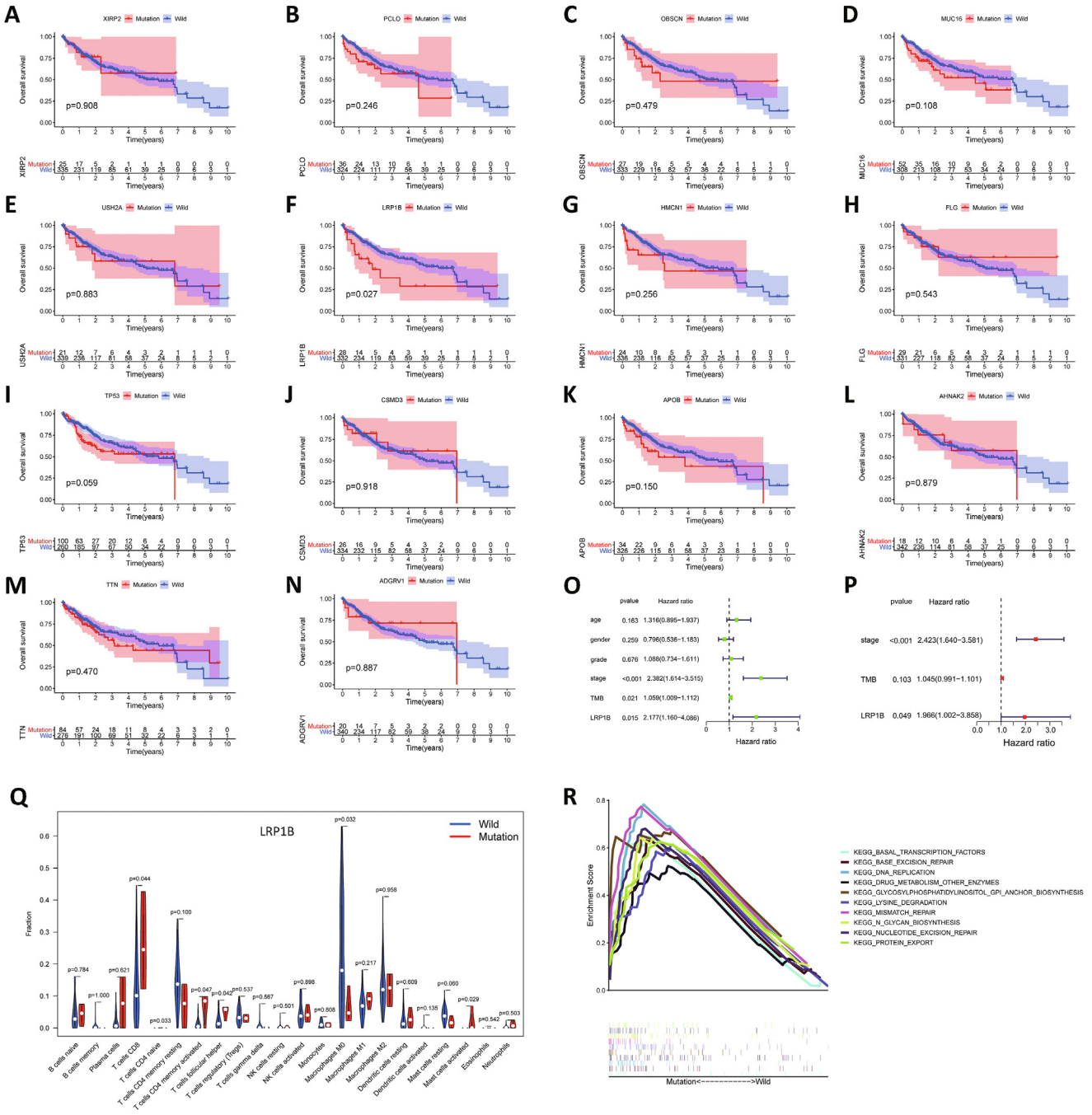

Figure 2 Prognostic analysis and immune cell infiltration analysis. **(A—N)** Survival curves of patients with mutant and wild-type genes: *XIRP2* (A), *PCLO* (B), *OBSCN* (C), *MUC16* (D), *USH2A* (E), *LRP1B* (F), *HMCN1* (G), *FLG* (H), *TP53* (I), *CSMD3* (J), *APOB* (K), *AHNAK2* (L), *TTN* (M) and *ADGRV1* (N). **(O)** Univariate Cox regression analysis. **(P)** Multivariate Cox regression analysis. **(Q)** Differential analysis of immune cell infiltration based on *LRP1B* mutation status (mutant or wild-type). **(R)** Gene set enrichment analyses (GSEA) based on *LRP1B* mutation status.

overexpression of *LRP1B* suppressed cell proliferation (Fig. 5A). The scratch migration assay results showed that overexpression of *LRP1B* suppressed the migration of HCCLM3 cells compared with that in the control group (Fig. 5B). In an experimental lung metastasis model established by tail vein injection, the number of lung metastases in mice injected with *shLRP1B* cells was significantly higher than that in mice injected with scramble control cells (Fig. 5C). Mice injected with *shLRP1B* cells exhibited a larger tumor volume and faster tumor growth ($P < 0.05$; Fig. 5D). Immunohistochemical analysis of subcutaneous tumors verified the *LRP1B* knockdown efficiency, and antigen KI-67 (*Ki-67*) staining was stronger in tumors formed from *shLRP1B* cells, indicating that the knockdown of *LRP1B*

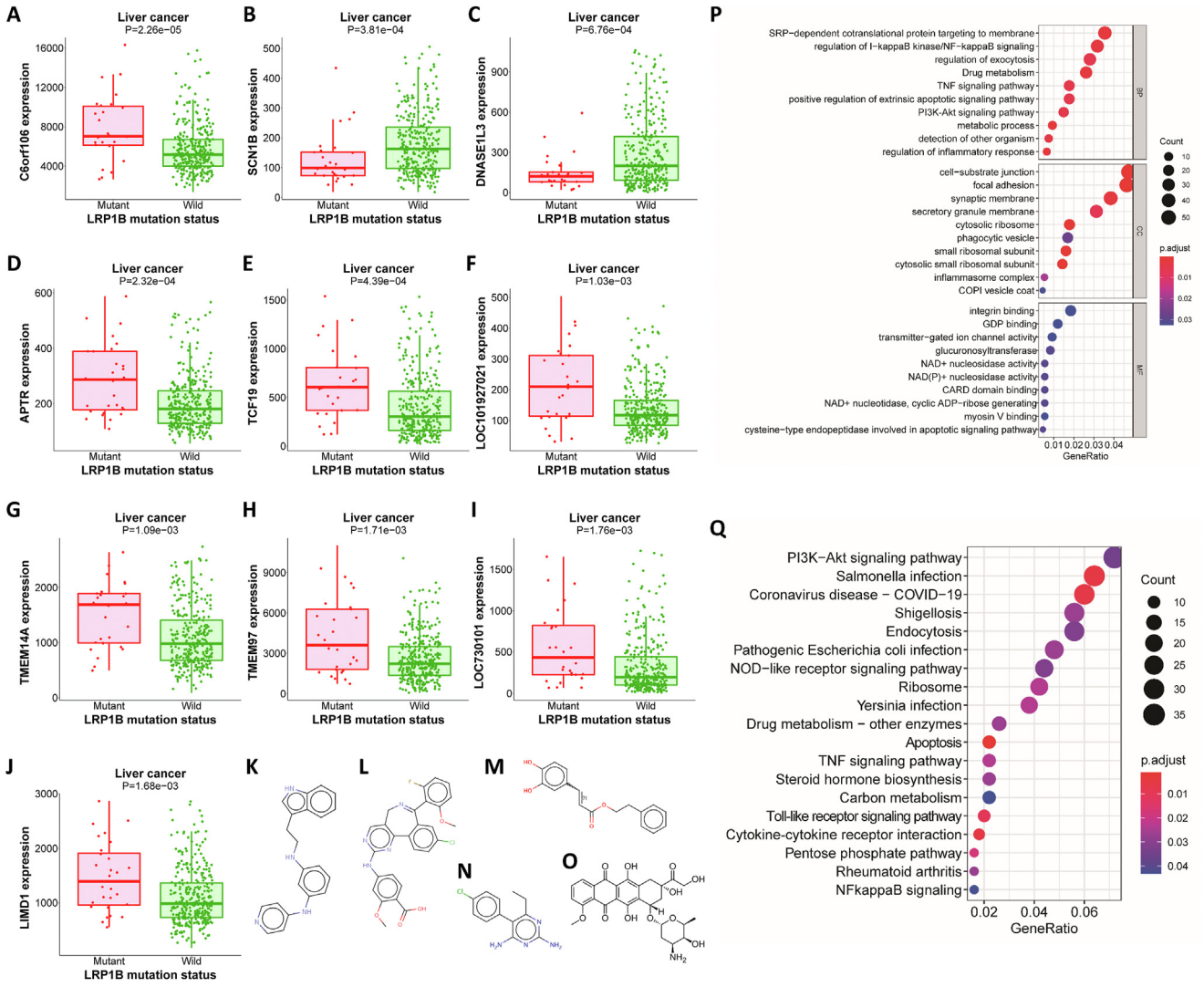

Figure 3 *LRP1B* mutation-related DEGs and functional enrichment analysis. **(A—J)** Expression levels of *f106* (A), *SCN1B* (B), *DNASE1L3* (C), *APTR* (D), *TCF19* (E), *LOC101927021* (F), *TMEM14A* (G), *TMEM97* (H), *LOC730101* (I) and *LIMD1* (J) in the *LRP1B* mutant and wild-type groups. **(K—O)** Molecular structure diagrams of serdemetan (K), alisertib (L), caffeic acid (M), pyrimethamine (N), and doxorubicin (O). **(P)** Gene ontology (GO) enrichment analysis. **(Q)** Kyoto Encyclopedia of Genes and Genomes (KEGG) enrichment analysis.

can promote tumor growth *in vivo* (Fig. 5E). Under doxorubicin treatment, the inhibition rate was calculated, and a dose—response curve was plotted. The half-maximal inhibitory concentration (IC_{50}) was calculated using GraphPad. The IC_{50} concentration was lowest in Huh7 cells among the tested cell lines, whereas the expression of *LRP1B* was the highest (Fig. 5F). The IC_{50} value in *LRP1B* knockdown cells was significantly higher than that in control cells ($P < 0.05$; Fig. 5G). Correspondingly, knockdown of *LRP1B* was verified to induce the resistance of tumor cells to liposomal doxorubicin in a mouse subcutaneous tumor model (Fig. 5H). Doxorubicin exerts an antitumor effect by inducing apoptosis[15] and enrichment analysis showed that *LRP1B* is related to apoptosis. Therefore, we examined the effect of *LRP1B* knockout on doxorubicin-induced apoptosis. Indeed, the knockout of *LRP1B* partially reversed liposomal doxorubicin-induced apoptosis (Fig. 5I).

LRP1B binds to *NCSTN* and regulates the PI3K/AKT/mTOR pathway

The KEGG enrichment analysis results suggested that *LRP1B* may be closely related to the PI3K/AKT signaling pathway. Western blot analysis confirmed that the knockdown of *LRP1B* significantly increased the phosphorylation levels of *PI3K*, *AKT*, and *mTOR* without affecting the corresponding total protein levels (Fig. 6A). Overexpression of *LRP1B* had the opposite regulatory effects on the PI3K/AKT/mTOR signaling pathway (Fig. 6B). *mTOR* is regulated by the AMPK/mTOR signaling pathway in addition to the PI3K/AKT signaling pathway; thus, we used the *AKT* phosphorylation inhibitor MK-2206. The results showed that *LRP1B* regulates *mTOR* through the PI3K/AKT signaling pathway but not the AMPK/mTOR signaling pathway (Fig. 6C). Co-IP and mass spectrometry analysis showed that *LRP1B* may directly bind

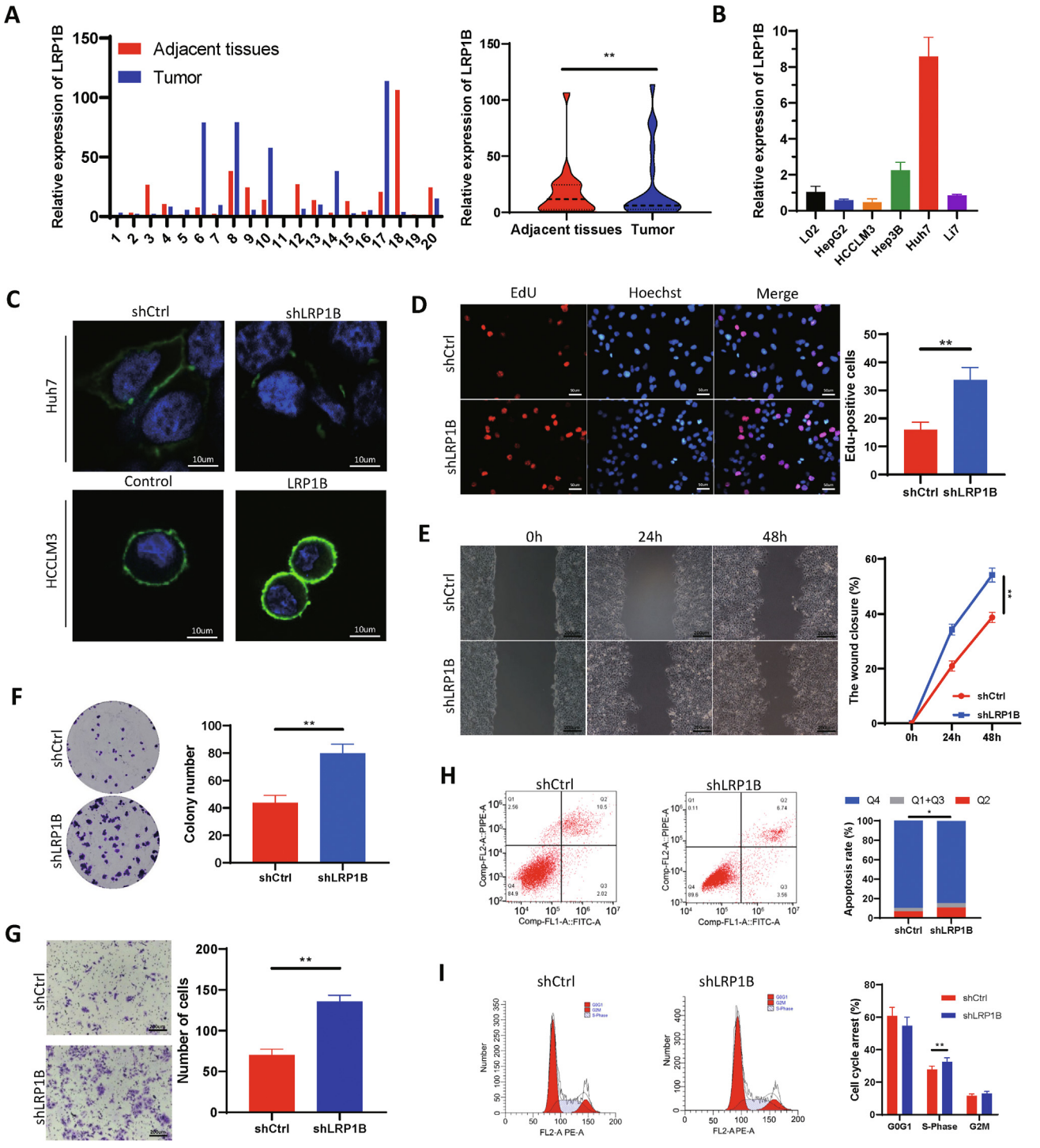

Figure 4 Low expression of *LRP1B* in hepatocellular carcinoma is associated with cell migration, proliferation, and apoptosis. **(A)** *LRP1B* expression was measured in adjacent and tumor tissues. **(B)** Relative mRNA expression of *LRP1B* in different cell lines. **(C)** Immunofluorescence staining for *LRP1B*. **(D)** EdU incorporation assay. **(E)** Scratch assay of Huh7 cells. **(F)** Plate colony formation assay. **(G)** Transwell migration assay. **(H)** Apoptosis was analyzed by flow cytometry. **(I)** The cell cycle distribution was analyzed by flow cytometry.

to *NCSTN*. We then performed co-IP experiments to verify the formation of the *LRP1B*/*NCSTN* protein complex in Huh7 cells (Fig. 6D). Furthermore, we carried out IP using lysates prepared from 293 T cells with exogenous overexpression of *LRP1B* and *NCSTN* and proved the reciprocal interaction between *NCSTN* and *LRP1B* (Fig. 6E, F).

LRP1B regulates the ubiquitination and protein level of *NCSTN*

We explored the influence of *LRP1B* on the degradation of the *NCSTN* protein by utilizing cycloheximide (CHX), which

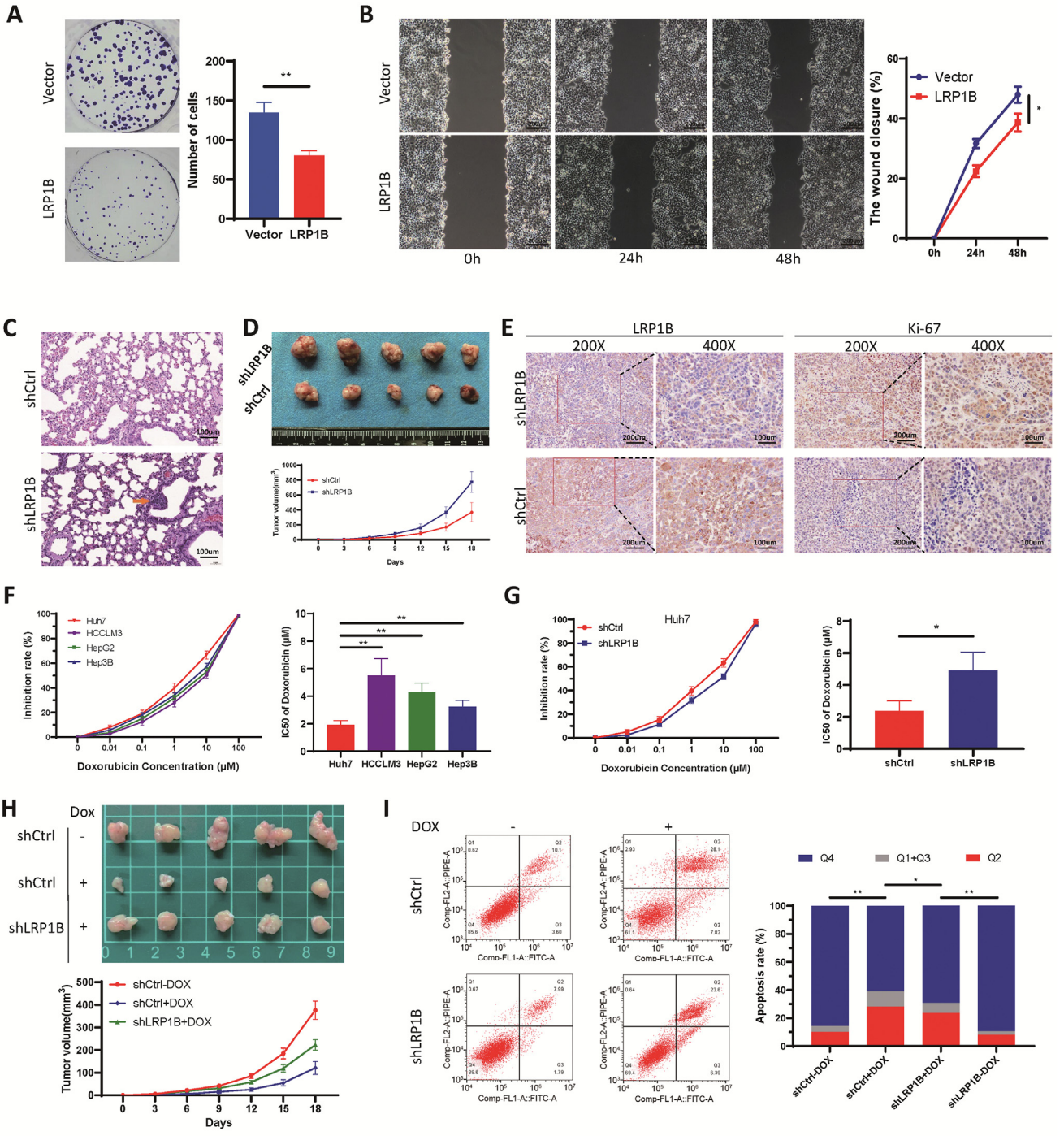

Figure 5 Effects of *LRP1B* on tumor progression and doxorubicin resistance. **(A)** Plate clone formation assay. **(B)** Scratch assay of HCCLM3 cells. **(C)** Lung metastatic foci in the lung metastasis model. **(D)** Photographs and growth curves of subcutaneous xenografts. **(E)** Immunohistochemical staining for the expression of *LRP1B* and *Ki67* in subcutaneous xenograft tissues. **(F)** IC_{50} values in different cell lines were determined based on 50% growth inhibition using a CCK-8 assay. **(G)** IC_{50} values were determined in *LRP1B* knockdown Huh7 cells and control cells. **(H)** Growth curves of subcutaneous xenografts treated with doxorubicin. **(I)** Detection of apoptotic Huh7 cells after doxorubicin and *shLRP1B* treatment.

can inhibit protein synthesis. After overexpression of *LRP1B* in HCCLM3 cells, the *NCSTN* protein degradation rate was accelerated compared with that in control cells, indicating that *LRP1B* promotes the degradation of *NCSTN* protein (Fig. 7A). To determine whether this clearance involves the proteasome pathway, we treated cells with MG132 to inhibit proteasomal degradation. The protein level of *NCSTN* increased gradually with prolonged MG132 treatment time, indicating that *NCSTN* could be degraded via the proteasome pathway (Fig. 7B). Overexpression of *LRP1B* decreased and knockdown of *LRP1B* increased the protein level of *NCSTN*, and these changes were reversed by MG132

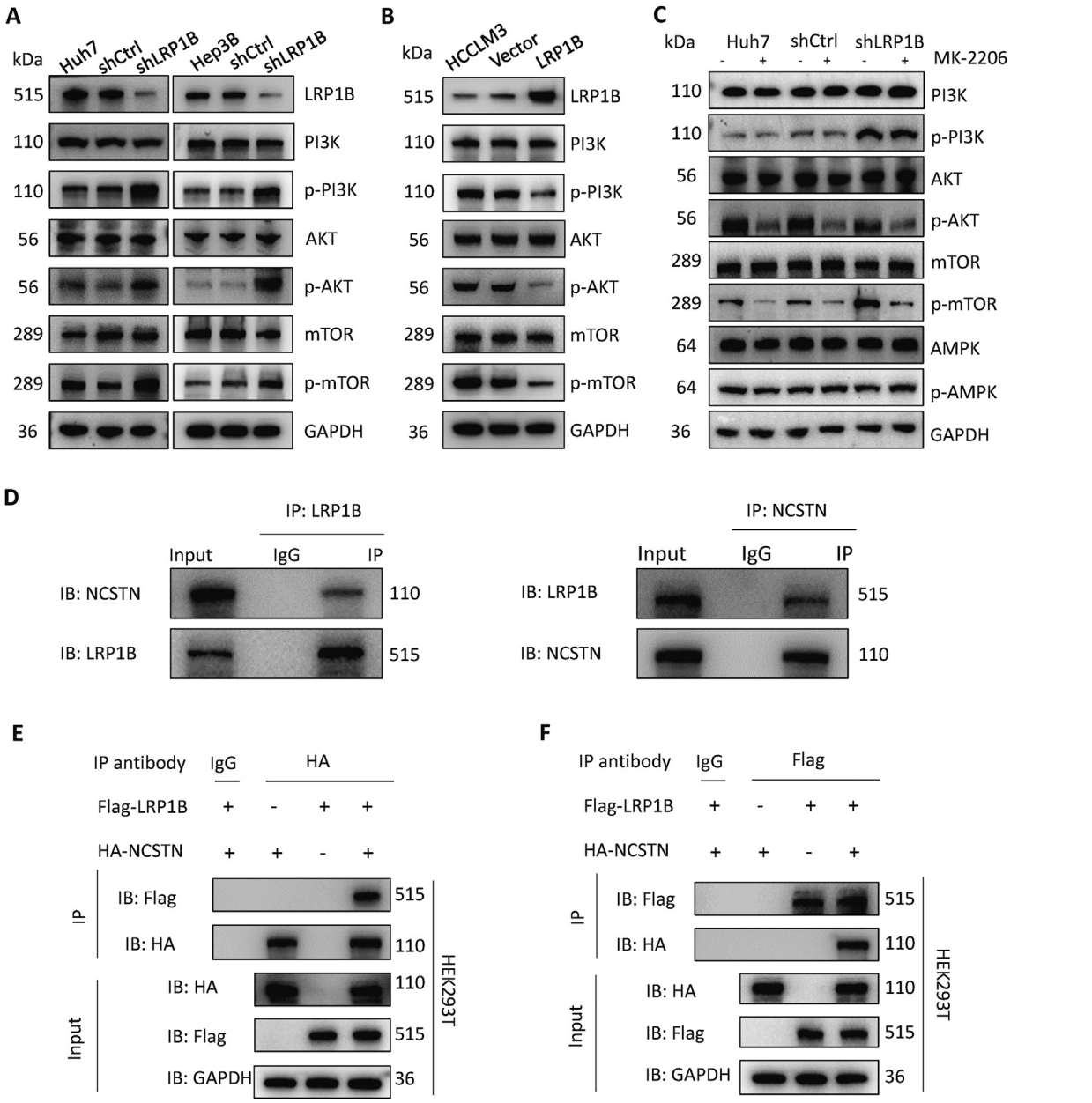

Figure 6 *LRP1B* directly binds to *NCSTN* and regulates the PI3K/AKT/mTOR pathway. **(A)** *LRP1B* knockdown causes upregulation of the PI3K/AKT pathway. **(B)** *LRP1B* overexpression inhibited the PI3K/AKT pathway. **(C)** *LRP1B* regulates the PI3K/AKT/mTOR pathway. **(D)** Immunoprecipitation (IP) assay in Huh7 cells. **(E)** IP assay in 293 T cells using a primary antibody specific for HA. **(F)** IP was performed with a primary antibody specific for Flag.

treatment (Fig. 7C, D). Overexpression of *LRP1B* increased the ubiquitination level of *NCSTN*; similarly, knockdown of *LRP1B* decreased the ubiquitination level of *NCSTN*, indicating that *LRP1B* can regulate the protein level of *NCSTN* by directly binding to *NCSTN* and promoting its ubiquitination and degradation (Fig. 7E).

LRP1B regulates the malignant behavior of HCC cells through the PI3K/AKT/mTOR signaling pathway

Previous studies have shown that *NCSTN* has a regulatory effect on the PI3K/AKT signaling pathway.[16,17] We performed rescue experiments to demonstrate that *LRP1B* plays a regulatory role in the malignant behavior of tumor cells through the PI3K/AKT pathway. The PI3K/AKT/mTOR pathway inhibitor MK-2206 and the agonist SC79 reversed the effect of *LRP1B* on the proliferation of Huh7 and HCCLM3 cells (Fig. 8A, B). The scratch assay showed that the promoting effect of *shLRP1B* on cell migration was reversed by MK-2206 treatment (Fig. 8C). Overexpression of *LRP1B* enhanced HCCLM3 cell apoptosis, an effect reversed by SC79 (Fig. 8D). Silencing *LRP1B* promoted cell proliferation in subcutaneous xenograft tissues in the mouse model, and this effect was reversed by MK-2206 treatment (Fig. 8E). Immunohistochemical assays were used to detect

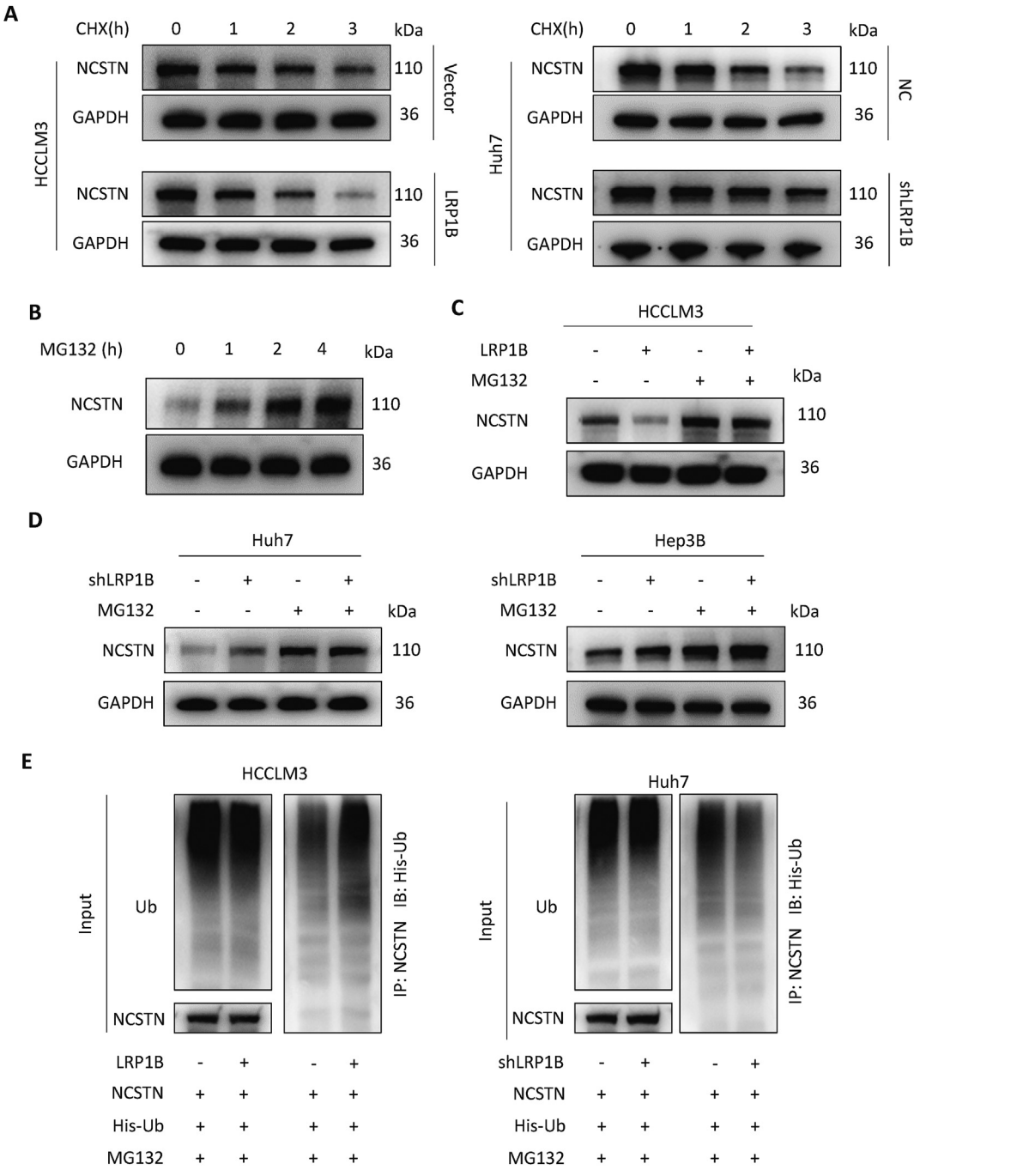

Figure 7 *LRP1B* regulates the ubiquitination, degradation, and protein level of *NCSTN*. **(A)** The rate of *NCSTN* degradation after cycloheximide (CHX) inhibition of protein synthesis. **(B)** *NCSTN* protein levels were determined after MG132 treatment. **(C)** The proteasome inhibitor MG132 restored the *LRP1B*-mediated reduction in the *NCSTN* protein level in cancer cells. **(D)** *LRP1B* regulates the ubiquitination of *NCSTN*.

the protein expression levels of *LRP1B* and *NCSTN*, and their expression was lower in tumors derived from shLRP1B cells than in tumors derived from control cells (Fig. 8F, G). In addition, the proportion of Ki-67-positive cells was significantly increased in tumors derived from shLRP1B-treated cells, and this increase was partially reversed by MK-2206 treatment (Fig. 8H). Oil Red O staining revealed that knockdown of *LRP1B* increased lipid droplet formation through the PI3K/AKT pathway and that this effect was reversed by MK-2206 treatment (Fig. 8I).

Discussion

HCC carcinogenesis is a complex multistep process involving multiple genetic mutations. The predominant consequence

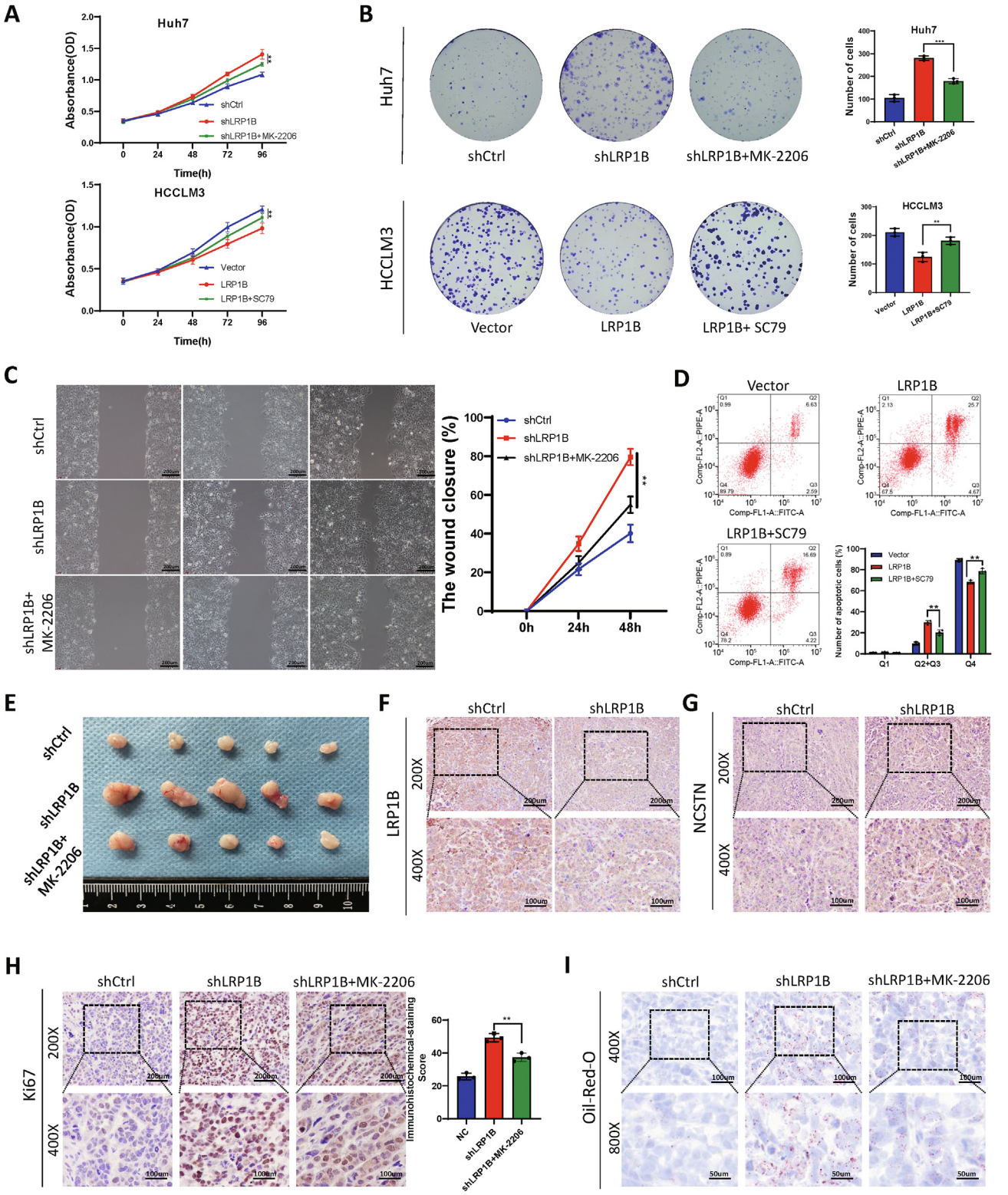

Figure 8 *LRP1B* regulates the malignant behavior of tumor cells through the PI3K/AKT/mTOR pathway. **(A)** Proliferation was evaluated by a CCK-8 assay. **(B)** Plate colony formation assays were used to detect cell proliferation. **(C)** Scratch assay. **(D)** Flow cytometry was used to detect apoptosis in transfected cells. **(E)** Subcutaneous xenografts in mice from the indicated groups. **(F, G)** Immunohistochemical staining for *LRP1B* (F) and *NCSTN* (G) in subcutaneous xenograft tissues. **(H)** Immunohistochemical staining for *Ki-67*. **(I)** Oil Red O staining of subcutaneous xenograft tissues.

of mutation accumulation is the activation of proto-oncogenes or silencing of tumor suppressor genes.[18] Somatic missense mutations strongly promote the generation of novel tumor epitopes. TMB can reflect the level of mutations in the exon-coding regions of genes in the genome. With the increasing use of immunotherapy in cancer patients, the study of TMB has attracted increasing attention. Generally, the higher the TMB, the greater the difference between tumor cells and normal cells, and the more likely the patient will benefit from immunotherapy. Therefore, the efficacy of immunotherapy in patients can be predicted according to the TMB. Associations between genetic mutations and TMB have previously been reported.[19] It is very important to study the relationship between single gene mutations, TMB, tumorigenesis mechanisms, and tumor therapy.

TMB and gene mutations were evaluated as potential biomarkers for immunotherapy and survival. However, studies investigating the relationship between TMB and genes with high mutation frequency in liver cancer are limited. Determining approaches to use effective biomarkers to identify immunotherapy-sensitive people has become a research hotspot. In this study, to further explore TMB-related gene mutations, we (i) counted and screened genes with high mutation frequency in liver cancer patients; (ii) analyzed differences in gene mutations between the high and low TMB groups; and (iii) identified a key mutated gene, *LRP1B*, associated with liver cancer prognosis. Through these studies, we identified *LRP1B* mutation as a key genetic mutation associated with TMB and patient prognosis.

LRP1B gene expression is frequently inactivated in numerous human malignancies, suggesting that this gene is a potential tumor suppressor gene. In our study, *TP53* was found to have the highest mutation frequency. The mutation frequency of *LRP1B* was lower than that of *TP53*, but survival analysis indicated that the *LRP1B* mutation had a stronger correlation with patient survival. Patients with *LRP1B* mutations had a significantly worse prognosis, indicating that *LRP1B* is a tumor suppressor gene with important functions and has important research value. We further analyzed the relationship between *LRP1B* and tumor immune cell infiltration and found that *LRP1B* mutation was associated with the infiltration of $CD8^+$ T cells. Inhibition of *PD-1/PD-L1* has been reported to increase the infiltration of $CD8^+$ T cells to kill tumor cells.[20] This observation suggests that mutations of *LRP1B* may be closely related to immunotherapy and may become an important immunotherapy target.

LRP1B, a member of the low-density lipoprotein (LDL) receptor family, is localized to the cell membrane, as shown by immunofluorescence. As a member of the LDL receptor family, *LRP1B* is involved in the uptake of anionic liposomes and drugs.[21,22] We identified doxorubicin, which is widely used in the treatment of liver cancer, by predicting the therapeutic effect of small molecule compounds. Based on this finding, we speculated that *LRP1B* might be involved in the uptake of liposomal doxorubicin. Similarly, previous studies have shown that *LRP1B* deletion in ovarian cancers is associated with resistance to liposomal doxorubicin.[23] We demonstrated that deletion of *LRP1B* in liver cancer cells is associated with resistance to liposomal doxorubicin by both *in vivo* and *in vitro* experiments. Mechanistically, *LRP1B* may bind to apolipoprotein E (*APOE*) in liposomes and participate in the uptake of liposomes. When *LRP1B* is knocked down, the uptake of liposomes is blocked; thus, doxorubicin cannot easily enter cells to exert its effects.

LRP1B participates in liposome uptake and regulates lipid metabolism in cells.[24–26] KEGG enrichment analysis indicated that *mTOR*, an important regulator of lipid metabolism, may also be regulated by *LRP1B*.[27,28] Therefore, we considered that *LRP1B* may regulate lipid metabolism in liver cancer cells through mTOR-related pathways. Subsequent experiments also confirmed the regulatory effect of *LRP1B* on the PI3K/AKT/mTOR pathway and revealed that the knockdown of *LRP1B* could activate *mTOR* to promote fat accumulation and liver cancer progression. Whether the *LRP1B* ectodomain binds to apoE-containing lipoproteins (high-density lipoprotein (HDL) and very-low-density lipoprotein (VLDL)) and is involved in lipoprotein uptake is worth investigating,[29,30] but inactivation of *LRP1B* ultimately leads to accumulation of intracellular lipids. Possible reasons are as follows: (i) lipoproteins and other ligands can induce other regulatory mechanisms mediated by the intracellular tail domain of *LRP1B*; and (ii) *LRP1B* and *LRP1* antagonize each other's functions by competing for the binding of common ligands, and the of *LRP1B* enables functional enhancement of *LRP1* with increased efficiency of lipoprotein endocytosis, thereby promoting cellular lipid uptake.[31] Therefore, the interaction between *LRP1B* and extracellular ligands and the biological function of the intracellular domain of *LRP1B* require further study.

LRP1B directly binds to *NCSTN* and decreases the *NCSTN* protein level. *LRP1B* is not a ubiquitinase, but it can increase the ubiquitination level of *NCSTN* to promote its degradation. Mechanistically, *LRP1B* may assist in recruiting a ubiquitinase for binding to *NCSTN*. Alternatively, *LRP1B* could compete with deubiquitinases for binding to the same binding site on *NCSTN*. Unfortunately, we have not determined the specific mechanism, and we will study it in depth in subsequent experiments.

This study has limitations. First, the data on gene mutations in liver cancer used in this study came from publicly available data and lacked the support of a large number of independent clinical samples. We plan to include clinical patient samples for gene sequencing in the future to further explore the types of gene mutations and the mutation frequency. Second, although this study showed that the *LRP1B* mutations are associated with immune cell infiltration in liver cancer, experimental validation is lacking. Finally, the specific site for the binding of *LRP1B* to *NCSTN* and the site and type of *NCSTN* ubiquitination were not determined.

In conclusion, this study demonstrates that mutations in *LRP1B* in liver cancer are associated with TMB and poor prognosis in patients. *LRP1B* mutation is associated with the infiltration of $CD8^+$ T cells in the immune microenvironment of liver cancer. Knockdown of *LRP1B* causes acquired resistance to liposomal doxorubicin in HCC cells. Inactivation of *LRP1B* can activate the PI3K/AKT/mTOR pathway in tumor cells to promote lipid accumulation, proliferation, invasion, and other malignant biological behaviors.

Therefore, our work revealed the important role and molecular mechanism of *LRP1B* in HCC progression, which may facilitate the development of immunotherapeutic approaches targeting *LRP1B*.

Author contributions

HZ, XL, and BJ designed the study and conducted the experiments and literature search. XYZ, ZX, GD, XLZ, and TX developed the methodology of analysis. XYZ, XLZ, DM, ZX, and GD helped with the collection and acquisition of data. XYZ, ZX, and GD analyzed the data. XYZ, ZX, XL, HZ, and BJ wrote the manuscript and revised the final version. All authors read and approved the final version of the manuscript.

Conflict of interests

The authors declare no conflict of interests.

Funding

This study was funded by the National Natural Science Foundation of China (No. 81871653), the Natural Science Foundation of Chongqing, China (No. cstc2020jcyj-msxmX0159), Chongqing Science and Health Joint Medical High-end Talent Project (China) (No. 2022GDRC012), Science and Technology Research Program of Chongqing Municipal Education Commission (China) (No. KJZD-K202100402 and KJQN201900449), CQMU Program for Youth Innovation in Future Medicine (China) (No. W0073) and Second Hospital of Shandong University Cultivation Funding(China) (No.2022YP45).

Appendix A. Supplementary data

Supplementary data to this article can be found online at https://doi.org/10.1016/j.gendis.2022.10.021.

References

1. Yang JD, Hainaut P, Gores GJ, et al. A global view of hepatocellular carcinoma: trends, risk, prevention and management. *Nat Rev Gastroenterol Hepatol*. 2019;16(10):589–604.
2. El-Serag HB, Rudolph KL. Hepatocellular carcinoma: epidemiology and molecular carcinogenesis. *Gastroenterology*. 2007;132(7):2557–2576.
3. Siegel RL, Miller KD, Jemal A. Cancer statistics, 2016. *CA Cancer J Clin*. 2016;66(1):7–30.
4. Riley TP, Keller GLJ, Smith AR, et al. Structure based prediction of neoantigen immunogenicity. *Front Immunol*. 2019;10:2047.
5. Brown LC, Tucker MD, Sedhom R, et al. *LRP1B* mutations are associated with favorable outcomes to immune checkpoint inhibitors across multiple cancer types. *J Immunother Cancer*. 2021;9(3):e001792.
6. Zheng H, Bai L. Hypoxia induced microRNA-301b-3p overexpression promotes proliferation, migration and invasion of prostate cancer cells by targeting LRP1B. *Exp Mol Pathol*. 2019;111:104301.
7. Wang Z, Sun P, Gao C, et al. Down-regulation of LRP1B in colon cancer promoted the growth and migration of cancer cells. *Exp Cell Res*. 2017;357(1):1–8.
8. Prazeres H, Torres J, Rodrigues F, et al. Chromosomal, epigenetic and microRNA-mediated inactivation of LRP1B, a modulator of the extracellular environment of thyroid cancer cells. *Oncogene*. 2011;30(11):1302–1317.
9. Lu YJ, Wu CS, Li HP, et al. Aberrant methylation impairs low density lipoprotein receptor-related protein 1B tumor suppressor function in gastric cancer. *Genes Chromosomes Cancer*. 2010;49(5):412–424.
10. Hong JY, Cho HJ, Kim ST, et al. Comprehensive molecular profiling to predict clinical outcomes in pancreatic cancer. *Ther Adv Med Oncol*. 2021;13:17588359211038478.
11. Cao CH, Liu R, Lin XR, et al. *LRP1B* mutation is associated with tumor HPV status and promotes poor disease outcomes with a higher mutation count in HPV-related cervical carcinoma and head & neck squamous cell carcinoma. *Int J Biol Sci*. 2021;17(7):1744–1756.
12. Wang L, Yan K, He X, et al. *LRP1B* or *TP53* mutations are associated with higher tumor mutational burden and worse survival in hepatocellular carcinoma. *J Cancer*. 2021;12(1):217–223.
13. Zhang Z, Cui R, Li H, et al. miR-500 promotes cell proliferation by directly targetting LRP1B in prostate cancer. *Biosci Rep*. 2019;39(4):BSR20181854.
14. Newman AM, Liu CL, Green MR, et al. Robust enumeration of cell subsets from tissue expression profiles. *Nat Methods*. 2015;12(5):453–457.
15. Mirzaei S, Zarrabi A, Hashemi F, et al. Nrf2 signaling pathway in chemoprotection and doxorubicin resistance: potential application in drug discovery. *Antioxidants*. 2021;10(3):349.
16. Xiao X, He Y, Li C, et al. Nicastrin mutations in familial acne inversa impact keratinocyte proliferation and differentiation through the Notch and phosphoinositide 3-kinase/AKT signalling pathways. *Br J Dermatol*. 2016;174(3):522–532.
17. Wang X, Wang X, Xu Y, et al. Effect of nicastrin on hepatocellular carcinoma proliferation and apoptosis through PI3K/AKT signalling pathway modulation. *Cancer Cell Int*. 2020;20:91.
18. Hahn WC, Weinberg RA. Rules for making human tumor cells. *N Engl J Med*. 2002;347(20):1593–1603.
19. Jia Q, Wang J, He N, et al. Titin mutation associated with responsiveness to checkpoint blockades in solid tumors. *JCI Insight*. 2019;4(10):e127901.
20. Kim HD, Song GW, Park S, et al. Association between expression level of PD1 by tumor-infiltrating $CD8^+$ T cells and features of hepatocellular carcinoma. *Gastroenterology*. 2018;155(6):1936–1950. e17.
21. Chung NS, Wasan KM. Potential role of the low-density lipoprotein receptor family as mediators of cellular drug uptake. *Adv Drug Deliv Rev*. 2004;56(9):1315–1334.
22. Lakkaraju A, Rahman YE, Dubinsky JM. Low-density lipoprotein receptor-related protein mediates the endocytosis of anionic liposomes in neurons. *J Biol Chem*. 2002;277(17):15085–15092.
23. Cowin PA, George J, Fereday S, et al. LRP1B deletion in high-grade serous ovarian cancers is associated with acquired chemotherapy resistance to liposomal doxorubicin. *Cancer Res*. 2012;72(16):4060–4073.
24. May P, Woldt E, Matz RL, et al. The LDL receptor-related protein (LRP) family: an old family of proteins with new physiological functions. *Ann Med*. 2007;39(3):219–228.
25. Masson O, Chavey C, Dray C, et al. LRP1 receptor controls adipogenesis and is up-regulated in human and mouse obese adipose tissue. *PLoS One*. 2009;4(10):e7422.
26. Haas J, Beer AG, Widschwendter P, et al. LRP1b shows restricted expression in human tissues and binds to several extracellular ligands, including fibrinogen and apoE - carrying lipoproteins. *Atherosclerosis*. 2011;216(2):342–347.

27. Mossmann D, Park S, Hall MN. mTOR signalling and cellular metabolism are mutual determinants in cancer. *Nat Rev Cancer*. 2018;18(12):744—757.
28. Caron A, Richard D, Laplante M. The roles of mTOR complexes in lipid metabolism. *Annu Rev Nutr*. 2015;35:321—348.
29. Strickland DK, Gonias SL, Argraves WS. Diverse roles for the LDL receptor family. *Trends Endocrinol Metabol*. 2002;13(2):66—74.
30. Shiroshima T, Oka C, Kawaichi M. Identification of LRP1B-interacting proteins and inhibition of protein kinase Cα-phosphorylation of LRP1B by association with PICK1. *FEBS Lett*. 2009;583(1):43—48.
31. Marzolo MP, Bu G. Lipoprotein receptors and cholesterol in APP trafficking and proteolytic processing, implications for Alzheimer's disease. *Semin Cell Dev Biol*. 2009;20(2):191—200.